Experimental advances in the quantum anomalous Hall effect

1). A. J. Bestwick, E. J. Fox, Xufeng Fu, Lei Pan, Kang L. Wang, and D. Goldhaber-Gordon, "Precise quantization of anomalous Hall effect near zero magnetic field," Phys. Rev. Lett. **114**, 187201 (2015)

2.) Cui-Zu Chang, Weiwei Zhao, Duk Y. Kim, Haijun Zhang, Badih A. Assaf, Don Heiman, Shou-Cheng Zhang, Chaoxing Liu, Moses H. W. Chan, and Jagadeesh S, Moodera, "High-precision realization of robust quantum anomalous Hall state in a hard ferromagnetic topological insulator", Nature Materials **14**, 473 (2015).

3.) Cui-Zu Chang, Weiwei Zhao, Duk Y. Kim, Peng Wei, J. K. Jain, Chaoxing Liu, Moses H. W. Chan, and Jagadeesh S. Moodera, "Zero-field dissipationless chiral edge transport and the nature of dissipation in the quantum anomalous Hall state", arXiv:1505.02306, Phys. Rev. Lett. (in press)

Recommended with a Commentary by Bertrand I. Halperin, Harvard University

In 2013, experimenters in Beijing [1] reported the first observations of the quantum anomalous Hall (QAH) effect, in a paper that earned a Journal Club Commentary by Leonid Glazman in July of that year. The three papers cited above describe impressive improvement in the quality of the quantized transport properties, and give important insight into the mechanisms for the remaining dissipation mechanisms at non-zero temperatures.

The QAH state resembles the ordinary integer quantized Hall effect in that it takes place in an essentially two-dimensional electron system, where the 2D bulk is insulating, (in the sense that the longitudinal conductivity σ_{xx} is =0, in the limit of zero temperature), but the Hall conductance of a sample is a non-zero and is quantized in units of e^2/h. Whereas the ordinary IQH effect requires application of a strong external magnetic field, however, the AQH can occur in zero magnetic field in a ferromagnet, where the necessary broken time-reversal symmetry can be produced by a uniform remnant magnetization. The difficulty and expense of producing the large magnetic fields necessary for the IQH state has been one huge obstacle to any possible practical application of the IQHE. However, the AQH requires only a relatively weak magnetic field, applied initially to produce a single-domain sample of the ferromagnet. Although other major obstacles to practical applications remain, the development of materials showing a high-quality AQH effect is certainly worthy of attention.

As in an IQH state, an AQH system has chiral electronic levels located at the sample edges, at the Fermi energy, which propagate in only one direction along the edge. If there are no other modes at the Fermi energy, then backscattering is impossible, and current can be carried along the edge with no dissipation at low temperatures, with a current-voltage relation that gives rise to the quantized Hall conductance.

However, a non-zero density of conducting states in the "bulk" of the material, or low-energy states near the edge that can propagate in the reverse direction, can lead to dissipation and inaccuracies in the quantized Hall conductance.

Broken time-reversal symmetry is necessary, but not sufficient, to produce a QAH state. The route to AQH employed in the systems under discussion use thin films of the three-dimensional topological insulator $(Bi_xSb_{1-x})_2Te_3$, doped with magnetic ions in sufficient concentration to produce a ferromagnetic sample. In the absence of broken time reversal, a 3D topological insulator will have conducting surface states, described in the simplest case by a single Dirac cone of states within the energy gap of the 3D bulk material. In the presence of an applied magnetic field or a ferromagnetic moment perpendicular to the surface, a gap may be opened up at the Dirac point, and if the Fermi level is adjusted to lie within this gap, the surface will become a quantized Hall conductor, with a Hall conductance given by $\pm e^2/2h$. For a thin film with a uniform magnetization perpendicular to the film, the two surfaces have the same Hall conductance and the sum of the two will produce a quantized Hall conductance of $\pm e^2/h$. A chiral edge state (which is also spin polarized) will then occur along the edge of the film, where the angle between the surface normal and the direction of magnetization passes through 90 degrees.

In the original experimental paper, [1], and in a later paper by a Japanese group [2], which was discussed in a Journal Club Commentary that I wrote in 2014, the magnetic ion employed was Cr, and the reported values of longitudinal resistivity, $\rho_{xx} = \sigma_{xx} / (\sigma_{xx}^2 + \sigma_{xy}^2)$, in zero magnetic field, were of the order of 0.5 h/e^2, or approximately 10^4 ohms.[3] By contrast, the first two papers reviewed in this Commentary have reported dramatic breakthroughs in materials preparation, which have led to longitudinal resistances below 10 ohms at their lowest temperatures.

The samples employed by Bestwick et al. (paper 1), in a Stanford-UCLA collaboration, were fabricated from films of $(Cr_{0.12}Bi_{0.26}Sb_{0.62})_2Te_3$, which were 10 quintuple layers thick, and grown on a GaAs substrate. The authors report values of the Hall resistance quantized to a part in 10^4 and longitudinal resistivities down to 1 ohm per square at the lowest temperatures, and they extract a thermal activation energy of 17 μeV (=200 mK) from an Arrhenius plot of the longitudinal conductivity at temperatures above 60 mK. Three terminal transport measurements showed a dramatic dependence on the direction of the remnant magnetization as would be expected for a QAH state, where the chirality of the edge channel depends on the magnetization direction.

The samples employed in paper 2 by Chang et al., (now part of an MIT, Penn State, Stanford, Northeastern collaboration), used V instead of Cr as the magnetic dopant. Results shown in the paper were obtained from a film of composition $(Bi_{0.29}Sb_{0.71})_{1.89}V_{0.11}Te_3$, which was 4 quintuple layers thick. This paper also reports a Hall conductance equal to the quantized value up to errors of a few parts in 10^4 and a zero-field longitudinal resistance of several ohms.

The new paper by Chang et al (paper 3) employs a V-doped sample similar to that of paper 2, in a set of measurements designed to shed light on the sources of remaining dissipation, including their dependence on temperature and back-gate voltage. Their measurements show that the dominant dissipation modes are different depending on whether the system is gated towards the electron rich or hole rich side of what they call a charge neutrality point. They infer that dissipation is due to bulk conduction channels on the hole rich side, but arises from extra non-chiral edge modes on the electron rich side. They illustrate their picture with the schematic band structure shown in Fig 1.
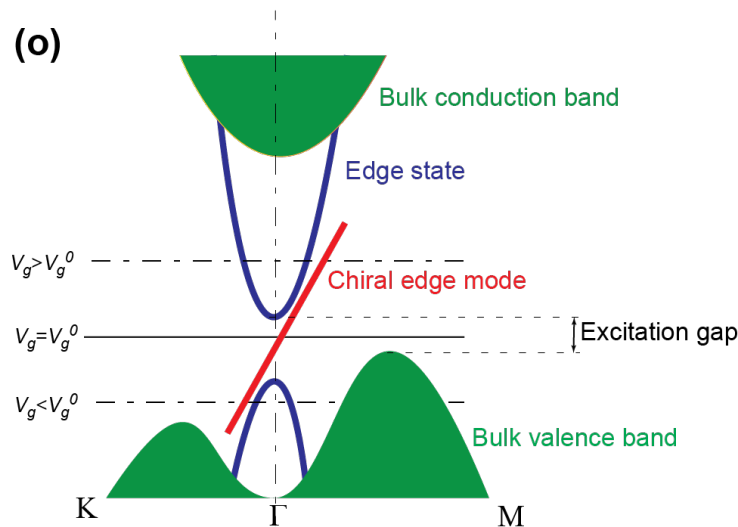

Figure 1. Schematic band dispersion of a single-crystal thin film of a ferromagnetic doped topological, showing bulk bands, a chiral edge mode, and non-chiral surface bands. Ferromagnetism is necessary to produce an energy gap between the upper and lower surface modes. For the indicated band structure, QAH occurs at low temperatures if the Fermi level falls in the excitation gap between the top of the bulk valence band and the bottom of the upper non-chiral surface band. The authors suggest that due to the reduction of the ferromagnetic gap near the edges, there may be a one-dimensional non-chiral band at the edge, pulled down from the 2D band, which may be still separated from the Fermi energy by a gap, but which can lead to non-chiral dissipative electron transport if carriers are excited into the band. As the ferromagnetic gap is likely to be reduced near the edges of the sample, there may be additional, non-chiral, edge modes, pulled out of the 2D surface bands, which can propagate.

The transport measurements were carried out using a sample with six contacts, as shown in Fig. 2 below. The authors use $\rho_{jk,lm}$ to denote the ratio of the voltage measured between contacts l and m to a current injected at contact j and removed at contact k. Measurements include two-point resistances, where contacts jk are the same as lm; four point measurements, where all contacts are different; and non-local three terminal measurements, where, say, $j=l$, but k and m are two other contacts. The colored arrows in Fig. 2 show how the opposite directions of chiral edge channels for positive and negative remnant magnetization affect their contributions to the current flow in a measurement of the non-local resistance $\rho_{26,35}$.
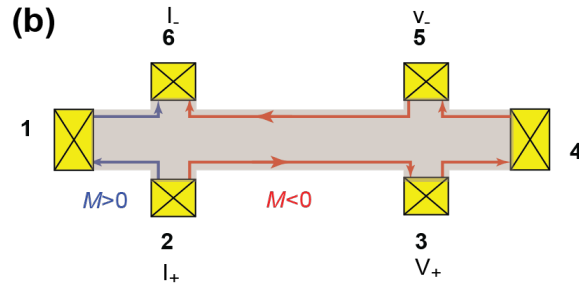

(b)

I$_-$ 6   V$_-$ 5

1   4

M>0   M<0

2   3

I$_+$ V$_+$

Figure 2: Geometry of sample contacts. Red and blue lines indicate current paths for $M<0$ and $M>0$ when current flows between contacts 2 and 6 via chiral edge states. Arrows show the chirality directions for the two cases.

The top panel of Fig. 3 shows results for the anomalous Hall resistance $\rho_{14,35}$ (red) and the longitudinal resistance $\rho_{14,23}$ (blue) at $B=0$ and $T=25$ mK, as a function of back gate voltage V_g. The middle panel shows the non-local resistance $\rho_{26,35}$ for the two directions of the remnant magnetization, while the ratio $\rho_{26,35}/\rho_{14,23}$ for $M>0$ is shown in the bottom panel. The differences in behavior between positive and negative values of V_g are striking, and the authors identify the charge neutrality point as $V_g^0 = +7$ V. The authors argue that for negative V_g, current flows between the contacts primarily through the bulk, leading to a large longitudinal resistance. The very small value of $\rho_{26,35}/\rho_{14,23}$ in this regime (of order 10^{-5}) is consistent with what one would expect for the non-local resistance in this geometry if the system were described by a bulk conductivity tensor that was largely independent of position. On the other hand, for positive V_g, the Hall resistance remains close to the quantized value h/e^2 and longitudinal resistance Hall resistance is close to zero over the indicated range. The non-local resistance is still small, but the ratio $\rho_{26,35}/\rho_{14,23}$ is now of order 10^{-2}. The authors' picture is that the current is largely carried by the chiral edge channel, but that there is leakage into non-chiral edge channels, which

can undergo back scattering and thereby lead to dissipation and non-quantized non-local resistance. Independent of details, the larger values of $\rho_{26,35}/\rho_{14,23}$, show that the current flow is concentrated near the edges, and is not consistent with what one would expect for bulk flow through a medium with a uniform conductivity tensor.
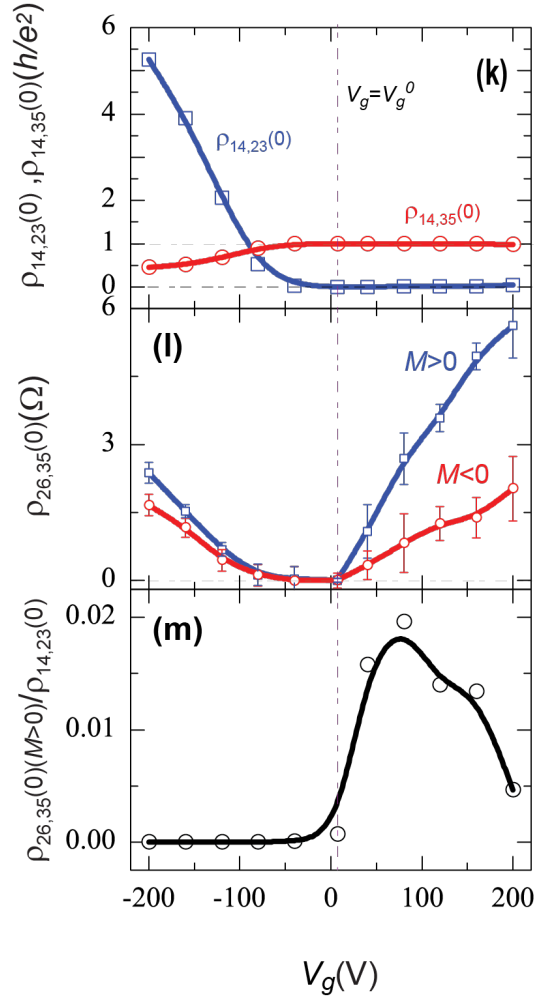
Figure 3: Four-terminal resistances as a function of gate voltage, at base temperature and $B=0$. Upper panel shows the longitudinal resistance (blue) and Hall resistance (red). Middle panel shows the non-local resistance $\rho_{26,35}$ for two directions of magnetization. Bottom panel shows the ratio $\rho_{26,35}/\rho_{14,23}$ for $M>0$.

The authors report results using other contact configurations, which give additional support to their picture. Measurements of the onset of dissipation with increasing temperature lead them to estimate an excitation gap $E_g = 50$ μV, which they identify

in the paper as the energy difference between the top of the bulk valence band and the bottom of the band of non-chiral edge modes, shown schematically in Fig. 1. (A more accurate interpretation is that the extracted value 50 μV is actually the distance between the Fermi level and the bottom of the non-chiral band, which should be only half the value of E_g.) In any case, the small values of the activation energies found here and in Bestwick, *et al.* explain why QAH effects are only observed at temperatures below about 100 mK in these materials, while ferromagnetism persists to much higher temperatures. (For example, a Curie temperature of 23K was quoted for the particular sample studied in paper 2.) A major challenge, now, is to find a way to increase the energy gaps, so that QAH could be observed at higher temperatures.

References:

[1]   C.-Z. Chang, J. Zhang, X. Feng, J. Shen, Z. Zhang, M. Guo, K. Li, Y. Ou, P. Wei, L.-L. Wang, Z.-Q. Ji, Y. Feng, S. Ji, X. Chen, J. Jia, X. Dai, Z. Fang, S.-C. Zhang, K. He, Y. Wang, L. Lu, X.-C. Ma, and Q.-K. Xue, "Experimental observation of the quantum anomalous Hall effect in a magnetic topological insulator," Science **340**, 167 (2013).

[2]   J. G. Checkelsky, R. Yoshimi, A. Tsukazaki, K. S. Takahashi, Y. Kozuka, J. Falson, M. Kawasaki, and Y. Tokura, "Trajectory of anomalous Hall effect toward the quantized state in a ferromagnetic topological insulator," Nature Physics **10**, 731 (2014).

[3]   See, also, X. Kou, *et al.*, Scale-invariant anomalous Hall effect in magnetic topological insulators beyond the two-dimensional limit," Phys. Rev. Lett. **113**, 137201 (2014).